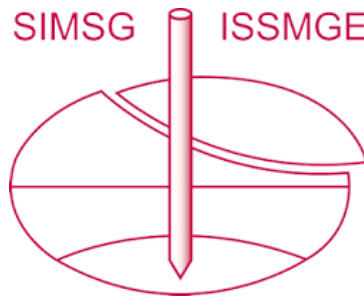


INTERNATIONAL SOCIETY FOR SOIL MECHANICS AND GEOTECHNICAL ENGINEERING



This paper was downloaded from the Online Library of the International Society for Soil Mechanics and Geotechnical Engineering (ISSMGE). The library is available here:

<https://www.issmge.org/publications/online-library>

This is an open-access database that archives thousands of papers published under the Auspices of the ISSMGE and maintained by the Innovation and Development Committee of ISSMGE.

The paper was published in the proceedings of the 20th International Conference on Soil Mechanics and Geotechnical Engineering and was edited by Mizanur Rahman and Mark Jaksa. The conference was held from May 1st to May 5th 2022 in Sydney, Australia.

An improved generalized scaling relation for dynamic centrifuge model tests

Une relation de mise à l'échelle généralisée améliorée pour les tests de modèles de centrifugeuses dynamiques

Yan-Guo Zhou, Qiang Ma, Di Meng & Yun-min Chen

Institute of Geotechnical Engineering, Zhejiang University, Hangzhou 310058, P. R. China, qzking@zju.edu.cn

ABSTRACT: Soil strain under dynamic loading is the key parameter to control the elasto-plastic deformation and even the failure processes. To overcome the defect that the strain of the model is always smaller than the prototype value in Iai's generalized scaling relations, an improved generalized scaling relation is proposed where the dynamic strain of model is designed to be equal to the prototype by modulating the amplitude and frequency of the input motion. Dynamic centrifuge model tests of dry sand are conducted with the same overall scaling factor ($\lambda=200$) under different centrifugal accelerations, to validate the improved generalized scaling relation. The test results of acceleration response, time histories of dynamic strains and ground settlements are analyzed, and it shows that the improved generalized scaling relation could achieve the same dynamic strain in models as that of the prototype, leading to a better physical modeling for geotechnical problems that dynamic strain of soil dominates the main response or the failure mechanism.

RÉSUMÉ : Une relation d'échelle généralisée améliorée est proposée. La relation de mise à l'échelle généralisée améliorée suppose que la déformation du sol sous une charge dynamique est le paramètre clé pour contrôler la déformation élastoplastique et même les processus de défaillance tels que l'initiation d'une pression interstitielle excessive. Pour surmonter le défaut selon lequel la déformation du modèle est toujours inférieure à la valeur du prototype dans les relations de mise à l'échelle généralisées de Iai, la déformation dynamique est conçue pour être égale au prototype dans la relation de mise à l'échelle généralisée améliorée en modulant l'amplitude et la fréquence du mouvement d'entrée. Une série de tests de modèles de centrifugeuses dynamiques de sable sec sont conduits avec le même facteur d'échelle global ($\lambda = 200$) sous différentes accélérations centrifuges, pour valider la relation d'échelle généralisée améliorée. Les résultats des tests de réponse à l'accélération, les historiques temporels des déformations dynamiques et les tassements au sol sont analysés, et cela montre que la relation de mise à l'échelle généralisée améliorée pourrait atteindre la même déformation dynamique dans les modèles que celle du prototype, conduisant à une meilleure modélisation physique pour la géotechnique. problèmes que la déformation dynamique du sol domine la réponse principale ou le mécanisme de défaillance.

KEYWORDS: Generalized scaling relation; centrifuge shaking table tests; dry sand; soil dynamic.

1 INTRODUCTION

Iai et al. (2005) developed a two-stage generalized scaling law (GSL) for centrifuge model tests that allows existing centrifuge facilities to model the response of much larger prototypes. The GSL has been applied widely in soil liquefaction (Tobita et al., 2011), dams and slopes (Park and Kim, 2017; Zhou et al., 2020), soil-structure interaction problems (Ueda et al., 2019) since it was proposed. One defect of GSL is that the scaling factor of shear strain is always larger than unity (i.e., $\lambda_\varepsilon > 1$). The scaling factor of strain should be unity in physical model tests, because soil strain under static or dynamic loading is the key parameter to control the elasto-plastic deformation and even the failure processes such as the initiation of excess pore pressure, the triggering of liquefaction, and the formation of strain localization in a boundary value problem. For instance, no excess pore water pressure will be accumulated in sandy soil when soil strain less than the threshold strain 0.01% (Dobry & Abdoun 2015). Although the induced shear strain in soil model subjected to dynamic loading is below the threshold strain and no excess pore pressure is observed, the corresponding prototype value might be higher than the threshold after being multiplied by λ_ε who is larger than unity. Then the build-up of excess pore pressure at prototype is expected and cyclic softening (or even liquefaction) will occur finally. This will lead to inconsistent result that the calculated response of the prototype is very different from that observed in model test (Zhou et al. 2020).

To address this issue, an improved generalized scaling relation is proposed in this paper. The dynamic strain of the model soil in the centrifuge model test is designed to be equal to the prototype by modulating the amplitude and frequency of the input motion. A suite of dynamic centrifuge model tests of

dry sand are conducted with the same overall scaling factor ($\lambda=200$) under different centrifugal accelerations by using the technique of "modeling of models", to validate the improved generalized scaling relation. Under a given centrifugal acceleration, sinusoidal input motion of 0.1g amplitudes and 1 Hz in prototype scale was applied to the model ground. The test results of acceleration response, time histories of dynamic strains and ground settlements are analyzed, and it shows that the improved generalized scaling relation could achieve the same dynamic strain in models as that of the prototype, leading to a better physical modeling for geotechnical problems that dynamic strain of soil dominates the main response or the failure mechanism.

2 BRIEF INTRODOCUTION OF THE IMPROVED GENERALIZED SCALING LAW.

According to Iai (1989), all scaling factors for physical model tests could be derived from the basic equations by using Buckingham's π theorem, and expressed in terms of some main factors. For a dry sand deposit, the behavior of dry sand is governed by the following equations:

Equilibrium:

$$\mathbf{L}^T \boldsymbol{\sigma} + \rho \mathbf{g} = \rho \ddot{\mathbf{u}} \quad (1)$$

Strain definition:

$$d\varepsilon = \mathbf{L} d\mathbf{u} \quad (2)$$

Constitutive law:

$$d\boldsymbol{\sigma} = \mathbf{D}d\boldsymbol{\varepsilon} \quad (3)$$

where $\boldsymbol{\sigma}^T=(\sigma_{11}, \sigma_{22}, \sigma_{33}, \tau_{12}, \tau_{23}, \tau_{31})$ is the stress, $\boldsymbol{\varepsilon}^T=(\varepsilon_{11}, \varepsilon_{22}, \varepsilon_{33}, \gamma_{12}, \gamma_{23}, \gamma_{31})$ is the strain, $\mathbf{u}^T=(u_1, u_2, u_3)$ is the displacement, \mathbf{D} is tangent modulus; $\mathbf{g}=(g_1, g_2, g_3)$ is the centrifugal acceleration; ρ is the soil density, and

$$\mathbf{L}^T = \begin{bmatrix} \frac{\partial}{\partial x_1} & 0 & 0 & \frac{\partial}{\partial x_2} & 0 & \frac{\partial}{\partial x_3} \\ 0 & \frac{\partial}{\partial x_2} & 0 & \frac{\partial}{\partial x_1} & \frac{\partial}{\partial x_3} & 0 \\ 0 & 0 & \frac{\partial}{\partial x_3} & 0 & \frac{\partial}{\partial x_2} & \frac{\partial}{\partial x_1} \end{bmatrix} \quad (4)$$

Introduce the scaling factors for the variables as:

$$\left. \begin{aligned} \mathbf{L}_p &= \lambda \mathbf{L}_m, \quad \boldsymbol{\sigma}_p = \lambda_\sigma \boldsymbol{\sigma}_m \\ \rho_p &= \lambda_\rho \rho_m, \quad \mathbf{g}_p = \lambda_g \mathbf{g}_m \\ \mathbf{u}_p &= \lambda_u \mathbf{u}_m, \quad t_p = \lambda_t t_m \end{aligned} \right\} \quad (5)$$

where the subscripts ‘‘p’’ and ‘‘m’’ indicate prototype and model respectively.

If the laminar container was used, the soil response could be reasonably considered as one-dimensional shear beam, Eq. (1) could be simplified into:

$$\left. \begin{aligned} \frac{\partial \tau_{31}}{\partial x_3} &= \rho \ddot{u}_1 \\ \frac{\partial \sigma_{33}}{\partial x_3} + \rho g_3 &= 0 \end{aligned} \right\} \quad (6)$$

and the scaling factor of shear strain λ_ε could be written as:

$$\lambda_\varepsilon = \lambda \lambda_a \lambda_\rho / \lambda_G \quad (7)$$

where λ represents the scaling factor of geometry; λ_ρ is the scaling factor of soil density; $\lambda_a = \lambda_{\ddot{u}_i}$ is the scaling factor of acceleration for input motion and λ_G is the scaling factor of tangent modulus.

If the modulus degradation behavior of soil is not considered, the scaling factor of shear modulus could be written as (Oztoprak & Bolton 2013):

$$\lambda_G = \frac{Af(e_p)\sigma_p^n}{Af(e_m)\sigma_m^n} \quad (8)$$

where A and n are material constant, $f(e)$ is a function of void ratio. For the case of $e_p=e_m$, Eq. (8) is simplified as:

$$\lambda_G = (\lambda_\sigma)^n = (\lambda \lambda_\rho \lambda_g)^n \quad (9)$$

where λ_σ is the scaling factor of stress and λ_g is the scaling factor of centrifugal acceleration.

Assume that $\lambda_\varepsilon=1$, and substitution of Eq. (9) into Eq. (7) we could derive:

$$\lambda_a = (\lambda \lambda_\rho)^{n-1} \lambda_g^n \quad (10)$$

If we scale down the amplitude of the input base motion according to Eq. (10), then $\lambda_\varepsilon=1$ could be achieved in the tests. The scaling relation of proposed generalized scaling law is summarized in Table 1.

Table 1. The scaling relation of proposed generalized scaling law

Items	Symbols	Scaling factors
Length	l	λ
Density	ρ	λ_ρ
Centrifugal acceleration	g	λ_g
Acceleration	a	$(\lambda_\rho \lambda)^{n-1} \lambda_g^n$
Time	t	$\lambda^{1-n/2} \lambda_\rho^{0.5-n/2} \lambda_g^{-n/2}$
Frequency	f	$\lambda^{n/2-1} \lambda_\rho^{n/2-0.5} \lambda_g^{n/2}$
Shear modulus	G	$(\lambda_\rho \lambda_g \lambda)^n$
Shear stress	τ	$(\lambda_\rho \lambda_g)^n \lambda^{1+n}$
Shear strain	ε	1
Overburden stress	σ	$\lambda \lambda_\rho \lambda_g$
Displacement	u	λ

3 CENTRIFUGE TEST.

3.1 Test material and test facilities

The sand material used in centrifuge model tests was Fujian sand, a typical fine silica sand with physical properties of $G_s=2.622$, $\rho_{\max}=1.638$ g/cm³, $\rho_{\min}=1.349$ g/cm³ and $D_{50}=0.16$. For sandy soil, there is a general acceptance of taking the value of ‘‘n’’ in Table 1 as 0.5 (Oztoprak & Bolton 2013).

The dynamic centrifuge tests were conducted on ZJU-400 centrifuge at Zhejiang University. (e.g., Zhou et al., 2020). The improved generalized scaling law proposed in Chapter 2 was adopted. The technique of ‘‘modeling of models’’ is used to validate the proposed improved generalized scaling law. Three models were designed with the same density and model geometries and the same overall length scaling factor ($\lambda=200$) under different centrifugal accelerations (12.5g for Model-A, 25g for Model-B and 50g for Model-C, respectively).

3.2 Model preparation

A laminar container was used and the inner dimensions of laminar container are 73 cm long, 33 cm wide and 42 cm high. Figure 1 details the model scale dimensions and sensor layout in model scale. The total depth of flat sand layer is 40 cm, corresponding to an 80-m-deep sand deposit in prototype scale. Six horizontal accelerometers (i.e. A1-A6) are located at the central array at the depth of 1 cm, 7.5 cm, 14 cm, 20.5 cm, 27 cm and 33.5 cm in model scale. One horizontal accelerometer was attached on the bottom of container to record the achieved base motion. Two laser displacement transducers (LDT) were installed at 18.5 cm and 54.5 cm from the left wall of the laminar container to monitor the settlements of model.

Air-pluviation method was used to prepare the flat model ground to secure a high level of soil uniformity. To minimize the effect of variation of dry sand density after each shaking event, the relative density of the flat ground is chosen as 95%. The target dry density of three models is $\rho_d=1.62$ g/cm³.

3.3 Test program and shaking sequences

The specified ground motion sequence includes nine destructive motions, each with a 1Hz sine wave for 30 cycles. The target peak base acceleration (PBA) was chosen to be 0.1g in prototype scale, which is corresponding to 5.0g for Model-A, 7.1g for Model-B and 10.0g for Model-C respectively in model scale. These tests were conducted under different centrifugal accelerations (i.e., 12.5g, 25g and 50g) to assess the behavior of a prototype through repetition of the test at different scales and comparison of the results in prototype scale.

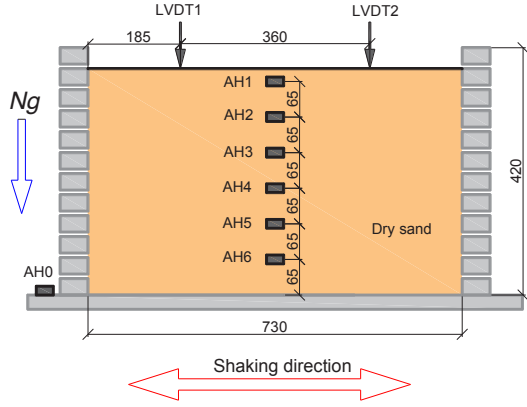


Figure 1. Side view of model instrumentations (model scale)

4 TEST RESULTS AND VALIDATION OF IMPROVED SCALING LAW.

4.1 Settlements

The density of dry sand might vary due to the destructive motions, which will have an uncertain effect on the validation of the improved scaling law. The total vertical settlements of the model during shaking events were less than 2 mm and the relative density of the model was only changed from 95% to 95.6%, which indicate that the density of dry sand was nearly constant during the shaking events. The shaking histories almost no effect on the validation of the improved scaling law.

4.2 Acceleration

The time histories of acceleration of three models are shown in Figure 2. The trends of three acceleration time histories show a high consistency: the shallower positions, the higher acceleration amplitude. The amplitudes of acceleration under the same depth are also nearly identical among three models, which shows that the proposed scaling law applies to acceleration response in the experiments.

To quantify the discrepancy of input motion, the method proposed by Goswami et al. (2017) was adopted in this study. Figure 3 illustrates the discrepancies of acceleration time histories among three models. Note the fact that the main discrepancy results from the phase lag induced by manually picking the starting time of time history under different centrifugal g -levels. The discrepancies in amplitude and frequency are trivial, the achieved amplitude and frequency under different centrifugal accelerations match well with each other, indicating almost identical acceleration response of three models.

4.3 Shear stress and strain

The shear strain of the upward propagating shear waves in nine destructive motions are estimated according to the procedure proposed by Zeghal et al (1999). The horizontal shear stress (τ_i) and the corresponding shear strain (γ_i) at elevation z_i could be expressed in Eqs. (11) and (12).

$$\tau_i(z_i, t) = \tau_{i-1}(t) + \rho \frac{\ddot{u}_{i-1} + \ddot{u}_i}{2} (z_i - z_{i-1}) \quad (11)$$

$$\gamma_i(z_i, t) = \frac{1}{(z_{i+1} - z_{i-1})} \left((u_{i+1} - u_i) \frac{z_i - z_{i-1}}{z_{i+1} - z_i} + (u_i - u_{i-1}) \frac{z_{i+1} - z_i}{z_i - z_{i-1}} \right) \quad (12)$$

where z_i refers to the depth of accelerometer A_i ($i=1$ to 6), \ddot{u}_i is the horizontal acceleration recorded by A_i . u_i is the displacement derived from the integration of acceleration record. The time history of shear strain at different depth of three model are shown in Figure 4. The trends and amplitudes of three shear strain time history show a high consistency for different strain levels, though the influence of modulus degradation is ignored. The results also confirm that the improved generalized scaling relation could achieve the same dynamic strain in models as that of the prototype.

The corresponding 19th to 21st shear stress-strain loops at different depths are shown in Figure 5, the shear stress-strain loops at prototype scale are almost identical under different centrifugal accelerations. It implies that the improved generalized scaling law works well for nonlinear dynamic response and the improved generalized scaling law could achieve similar shear stress-strain behavior between models and prototype.

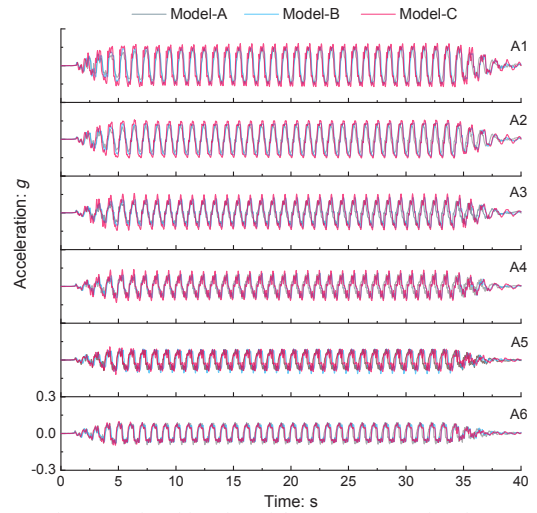


Figure 2. Time histories of the response accelerations

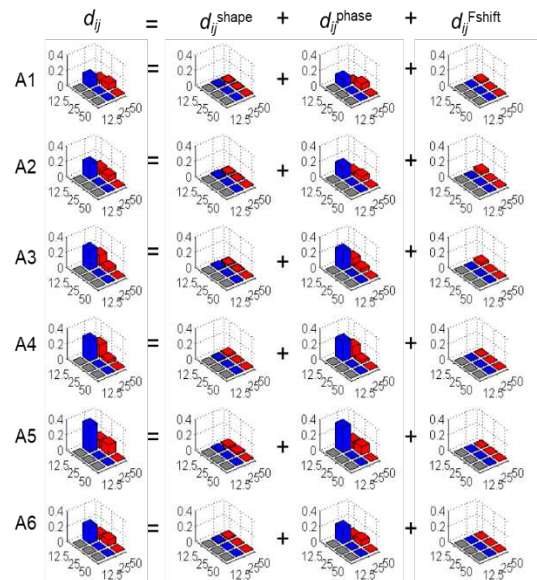


Figure 3. The discrepancies of acceleration time histories

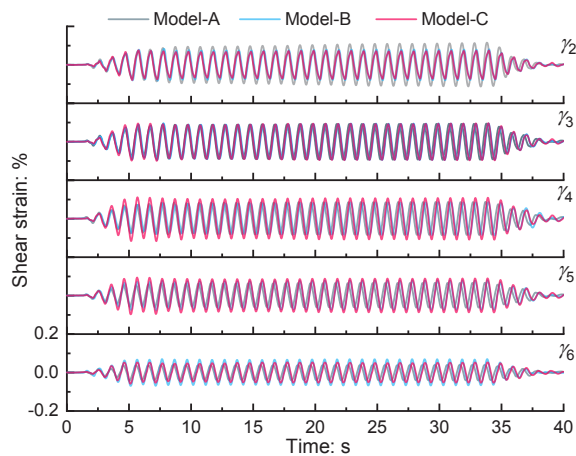


Figure 4. Comparison of shear strain for three models

5 CONCLUSIONS

In this study, to overcome the defect that the strain of the model is always smaller than the prototype value in Iai's generalized scaling relations, the strain of the model soil in dynamic centrifuge model test is designed to be equal to the prototype in the improved generalized scaling relation by modulating the amplitude and frequency of the input motion. A suite of dynamic centrifuge model tests of dry sand are conducted with the same overall scaling factor ($\lambda=200$) under different centrifugal accelerations by using the technique of "modeling of models", to validate the improved generalized scaling relation. Under a given centrifugal acceleration, sinusoidal input motion was applied to the model ground. The main findings of this study include:

- The total vertical settlements of the model during shaking events were less than 2 mm and the relative density of the model was only changed from 95% to 95.6%. The shaking histories almost no effect on the validation of the improved scaling law.
- The amplitudes of acceleration under the same depth are nearly identical among three models, which shows that the proposed scaling law applies to acceleration response in the experiments.
- The amplitudes of shear strain under the same depth are also agree with each other, which confirms that the improved generalized scaling relation works well for nonlinear dynamic response and could achieve the same dynamic strain in models as that of the prototype.

6 ACKNOWLEDGEMENTS.

This study is supported by the National Natural Science Foundation of China (Nos. 51988101, 51978613, 51778573) and the Chinese Program of Introducing Talents of Discipline to University (the 111 Project, B18047).

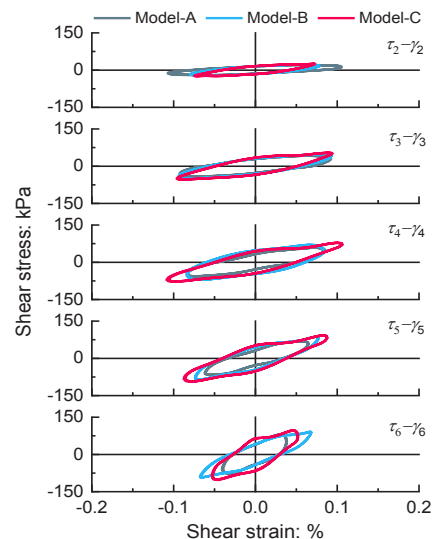


Figure 5. Stress-strain loops for three models

7 REFERENCES.

- Dobry R. and Abdoun, T. 2015. Cyclic shear strain needed for liquefaction triggering and assessment of overburden pressure factor $K\sigma$. *Journal of Geotechnical and Geoenvironmental Engineering*, 141 (11), 04015047.
- Goswami N., Zeghal M., Manzari, M. et al. 2017. Metrics for the Comparison of Acceleration Time Histories. In proceeding of Geotechnical Frontiers, ASCE, pp. 215–224.
- Iai S. 1989. Similitude for shaking table test on soil-structure-fluid model in 1g gravitational field. *Soils and Foundations*, 29(1), 105–118.
- Iai S., Tobita T. and Nakahara T. 2005 Generalized scaling relations for dynamic centrifuge tests. *Geotechnique*, 55(5), 355–362.
- Oztoprak S. and Bolton M.D. 2013. Stiffness of sands through a laboratory test database. *Geotechnique*, 63(1), 54–70.
- Park, D.S., Kim, N.R. 2017. Safety evaluation of cored rockfill dams under high seismicity using dynamic centrifuge modeling. *Soil Dynamics and Earthquake Engineering*, 97: 345–363.
- Tobita T., Iai S., Tann L. Yaoi Y. 2011. Application of the generalized scaling law to saturated ground. *International Journal of Physical Modelling in Geotechnics*, 11(4): 138–155.
- Ueda K., Sawada K., Wada T., Tobita T., Iai S. 2019. Applicability of the generalized scaling law to a pile-inclined ground system subject to liquefaction-induced lateral spreading. *Soils and Foundations*, 59: 1260–1279.
- Zeghal M., Elgamal A.W., Tang H.T. and Stepp J.C. 1995. Lotung downhole array II: evaluation of soil nonlinear properties. *Journal of Geotechnical Engineering*, 121 (4), 363–378.
- Zhou Y.G., Sun Z.B. and Chen Y.M. 2016. Curved raypaths of shear waves and measurement accuracy of bender elements in centrifuge model tests. *Journal of Geotechnical and Geoenvironmental Engineering*, 142 (6), 04016008.
- Zhou Y.G., Meng D., Ma Q., Ling D.S., Huang B. and Chen Y.M. 2020. Frequency response function and shaking control of the ZJU-400 geotechnical centrifuge shaker. *International Journal of Physical Modelling in Geotechnics*, 20(1), 97–117.
- Zhou Y.G., Meng D., Ma Q. Huang B., Ling D.S., Chen Y.M. 2019. Centrifuge modeling of dynamic response of high fill slope by using generalized scaling law. *Engineering Geology*, 260: 105213.